

Optically active three-dimensionally confined structures realized via molecular beam epitaxial growth on nonplanar GaAs (111)B

K. C. Rajkumar, A. Madhukar, K. Rammohan, D. H. Rich, P. Chen, and L. Chen
*Photonic Materials and Devices Laboratory, Department of Materials Science and Engineering,
University of Southern California, Los Angeles, California 90089-0241*

(Received 4 June 1993; accepted for publication 21 September 1993)

We report the first realization on *nonplanar* patterned substrates of optically active *three-dimensionally* confined semiconductor volumes created *in situ* via a one-step molecular beam epitaxial growth. Growth is carried out on pyramidal mesas on (111)B substrates and in a regime that results in the emergence of three equivalent {110} side facets which overtake the as-patterned {100} side facets and lead to mesa pinch-off. Transmission electron microscopy along with spatially and spectrally resolved cathodoluminescence provide evidence for emission from laterally confined regions with lateral linear dimensions $\lesssim 100$ nm.

Structures with the electronic states confined in all three dimensions termed quantum dots (QDs) have become the subject of increasing interest.¹ Conventional, postgrowth lithographic approaches to carve out such structures in as-grown usual quantum wells having confinement in the growth direction alone continue to pose difficulties *vis a vis* the induced damage and the concomitant loss of optical emission.² Alternatively, synthesis of such structures via purely growth steps³⁻⁵ offers the potential for circumventing these limitations. Here we report evidence for the first realization of optically active three-dimensionally confined GaAs volumes grown on *nonplanar* patterned substrates via molecular beam epitaxy (MBE). The growth is on pyramidal mesas etched on GaAs (111)B substrates. The *in situ* approach employed here involves growth of a buffer on a mesa with starting mesa top linear dimensions of the order of a micron with the objective of shrinking its size down to the quantum confinement regime (< 500 Å) followed by the deposition of a nominal quantum well (QW).^{4,6} The QW is then buried under the higher band gap material from all sides and leads to a QD. A sufficient requirement for such a size-reducing epitaxial growth is a net migration into the mesa top⁴⁻⁶ from the preexisting or self-generated sidewalls.

Truncated triangular-base pyramidal mesas having {100} sidewalls and top lateral dimensions $\lesssim 1$ μm were created using patterning by conventional photolithography followed by wet chemical etching of (111)B GaAs substrates ($\pm 0.1^\circ$).^{4,5} The substrates then were subjected to the standard substrate cleaning procedure prior to growth in a Perkin-Elmer ϕ -400 MBE machine. The growth conditions were set at arsenic pressure of 1.2×10^{-6} Torr, substrate temperature of 635 °C and a GaAs growth rate of 0.4 ML/s. The nominal structure of the sample discussed here consists of a 5 ML $\text{Al}_{0.2}\text{Ga}_{0.8}\text{As}$ marker deposited upon deoxidation of the fresh substrate, 115 ML GaAs buffer layer to stabilize the (111)B surface,⁷ a 918 ML size-reducing layer, a four-period 30 ML $\text{Al}_{0.2}\text{Ga}_{0.8}\text{As}$ /20 ML GaAs multiple quantum well (MQW) and finally a 150 ML cap (1 ML = 3.26 Å). In order to follow the evolution of the growth front, the buffer and cap layers were marked by 5 ML $\text{Al}_{0.2}\text{Ga}_{0.8}\text{As}$ layers every 46 ML of GaAs.

Figure 1 is a scanning electron microscope (SEM) image of a typical mesa after the growth. The threefold sym-

metry of the *as-patterned* mesa is retained. All the mesas in the 5 mm square patterned field containing mesa top linear dimensions ranging from 0.5 to 1.1 μm were found to have pinched off. Three facets (marked by black arrow in Fig. 1) making an angle of 35° with the (111)B plane have evolved and are identified to be equivalent {110} planes. Lower on the mesa other facets (marked by A) not contiguous with the (111)B top have evolved between the {100} planes. The lower arsenic pressure and higher substrate temperature than that used in our previous work (Refs. 4 and 5) have favored the evolution of {110} planes over {211} planes. Our experience indicates this to be a more controllable approach, apart from giving more effective electronic confinement.

Figure 2 is a {200} dark field cross-sectional transmission electron microscope (TEM) image along a $\langle 01\bar{1} \rangle$ azimuth (white arrow in Fig. 1) of a typical mesa. The bright AlGaAs marker layers reveal the evolution of the lateral dimensions of the (111)B mesa top layers. The *as-patterned* mesa top size of 1.05 μm , as measured by the length of the first AlGaAs marker layer, reduces to an apex in the cap layer. The (111)B layers are bounded on the left side of the TEM image by a {110} sidewall. Under the azimuth of imaging, the other two {110} sidewalls are not parallel to the e^- beam and, hence, are not imaged. On rotating the TEM specimen about $\langle 111 \rangle$ through 60° , one of these two {110} sidewalls align along the e beam. It is

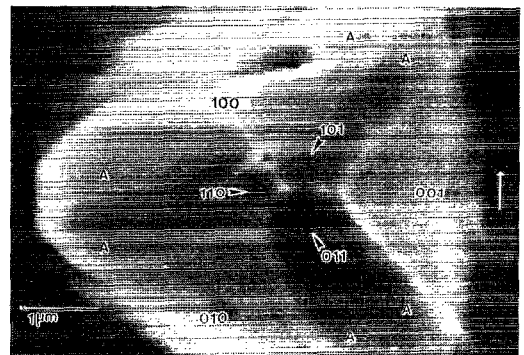


FIG. 1. SEM image after growth on a truncated pyramidal (111)B mesa. The (111)B mesa top has pinched off into an apex after growth.

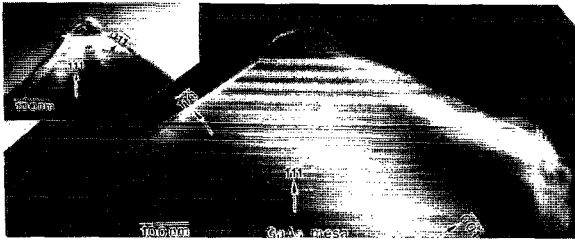


FIG. 2. Dark field $\{200\}$ reflection $\langle 01\bar{1} \rangle$ azimuth TEM image of a pinched off mesa showing its inner structure. AlGaAs (bright); GaAs (dark). $\{110\}$ side facet appears on the left side of the $(111)B$ layers. Inset shows the same mesa with a rotation of 60° about $[111]$ to view along another $\langle 01\bar{1} \rangle$ azimuth. $\{110\}$ side facet appears on the right side.

then imaged (inset of Fig. 2) on the right side of the $(111)B$ layers. The GaAs wells in the MQW are thus confined in the vertical direction by the $(111)B$ AlGaAs layers and from all lateral directions by the $\{110\}$ AlGaAs layers. The emergence of, and the lack of growth on, the $\{110\}$ sidewalls surrounding the QWs is a feature of fundamental significance to the realization of confinement of carriers (electrons and holes) and is quite different from our earlier scheme (Ref. 4) of *in situ* realization involving $\{211\}$ sidewalls. The nonzero growth on the $\{211\}$ sidewalls placed the burden of the lateral confining potential on the difference in the electronic levels of the GaAs wells of differing thicknesses on the $\{211\}$ sidewalls and the (111) mesa top. In the present case, superior lateral confining potential barriers resulting from the absence of growth on GaAs on the $\{110\}$ sidewalls are achieved and are manifest in the optical emission behavior discussed in the following. Also, the near-zero growth on $\{110\}$ results in the rate of shrinkage with growth on the $(111)B$ layers to be equal to the crystallographic angle between the two planes. This renders the design of a structure to result in mesa pinch-off at a predetermined quantum well easier than in the case of mesas with $\{211\}$ sidewalls. The nonzero growth on $\{211\}$ planes results in the rate of shrinkage to be uncoupled to the crystallographic angle between the $\{211\}$ and $(111)B$ planes and thus sensitive to small variations in the growth conditions.

The smallest QW in Fig. 2 has lateral dimensions of 1800 \AA (bottom) and 1400 \AA (top), is 117 \AA thick, and is located 350 \AA below the pinch-off point. The four QW thicknesses are within 32 ± 2 ML. However, the as-deposited 46 ML GaAs increments constituting the superlattice (SL) buffer layer show a dramatic thickness variation. For the first few periods only 2–3 MLs grow on the mesa top. A steady increase in the GaAs thickness occurs in subsequent depositions, reaching 61 MLs for the 18th deposition. This can be understood on the basis of a highly nonlinear net atom migration as a function of the changing mesa size in relation to the effective migration length.^{4,8} For the initial periods, the $(111)B$ mesa top layer is in contact with the layers growing on the *as-patterned* three equivalent $\{100\}$ side facets. Adatom migration initially occurs from the $(111)B$ mesa top to the $\{100\}$ facets [as has been observed to occur from the $(111)B$ side facets

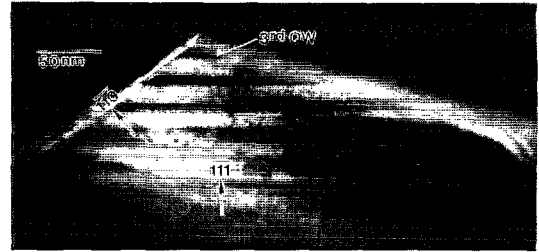


FIG. 3. Dark field $\{200\}$ reflection $\langle 01\bar{1} \rangle$ azimuth TEM image of a $0.6 \mu\text{m}$ mesa.

onto (100) mesa top for striped (100) mesas (Ref. 9)] resulting in near-zero thicknesses on the mesa top and an increasing mesa top dimension. Concomitantly, three equivalent $\{110\}$ facets emerge. However, from these facets also, almost complete migration occurs into the adjacent $\{100\}$ facets as seen in the near-zero growth on $\{110\}$. A consequence is that the length of the segments along which the $(111)B$ layer meets the $\{100\}$ layers shrink, eventually reducing to zero. Beyond this $\{100\}$ pinch-off point, there results a net migration from the $\{110\}$ facets into the $(111)B$ mesa top, which they now completely surround. Initially, this results in the $(111)B$ layers becoming increasingly thicker than that deposited while shrinking in lateral dimensions. However, when the mesa top dimension becomes comparable to the $(111)B$ intraplanar migration length, the net flow rate into the mesa top becomes nearly constant. Thus, near the pinch-off region the layer thicknesses become nearly constant as seen for the four quantum wells at the top (Fig. 2).

Figure 3 is a cross-sectional TEM image of the growth on a $0.6 \mu\text{m}$ *as patterned* mesa. Pinch-off has occurred at the fourth QW. The third three-dimensional QW has lateral dimensions of 1116 \AA (bottom) and 716 \AA (top) and is 84 \AA thick. The fourth quantum well is not seen in this image as it has unfortunately been milled away during TEM specimen preparation. However, given the inclination of the $\{110\}$ sidewalls and the observed dimensions of the third well we can reliably estimate that the mesa pinch-off has occurred in the fourth well and provides a pyramidal volume bounded by a base of 324 \AA and height 65 \AA . Finally, in Fig. 3, a very thin sidewall growth is observed. The near absence of the material deposited beyond the pinch-off point indicates that it has migrated onto the facets labeled A in Fig. 1.

Figure 4(a) presents two areally averaged CL spectra, one from the reference unpatterned region and the other from the patterned region containing predominantly $0.6 \mu\text{m}$ mesas. The 832 nm peak corresponds to the C-acceptor level in bulk GaAs. The remaining peak positions were compared against calculated values for the four QWs and the buffer on $(111)B$ with the assumption of a 65:35 rule for the band offsets and a 6 meV exciton binding energy. For the unpatterned region, the observed peaks at 789 and 812 nm coincide well with the calculated values of 789.8 nm for a 20 ML GaAs/ $\text{Al}_{0.2}\text{Ga}_{0.8}\text{As}$ QW and 812.9 nm for a 46 ML GaAs/5 ML $\text{Al}_{0.2}\text{Ga}_{0.8}\text{As}$ SL, respectively. For

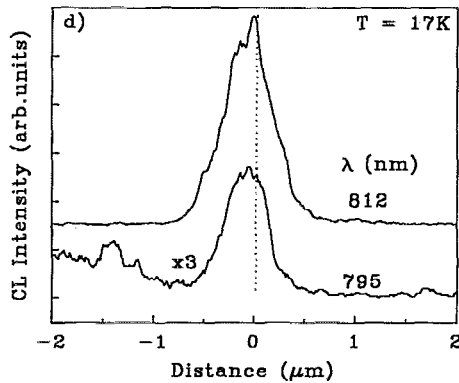
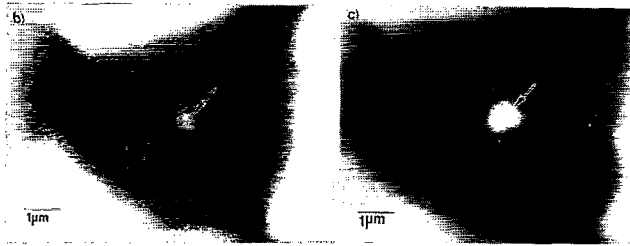
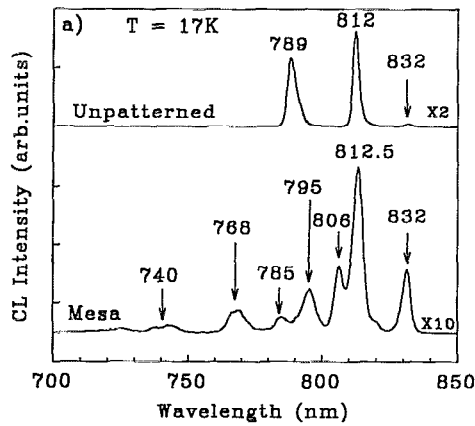


FIG. 4. (a) Area averaged CL spectra from unpatterned region ($64 \times 48 \mu\text{m}^2$) and mesa ($2.6 \times 1.9 \mu\text{m}^2$). (b) CL image at 795 nm. (c) CL image at 812 nm. (d) Histograms at 795 and 812 nm. The origin on the x axis coincides with the position of the mesa apex transferred onto the CL image from a simultaneously acquired SEM image. Uncertainty in apex determination is $\pm 0.1 \mu\text{m}$.

the mesa region, *simultaneous* acquisition of the CL and secondary electron signals allowed unambiguous determination of the spatial origin of the emission by circumventing instrumental complications such as vibration and possible sample thermal drift during data acquisition.

The mesa peaks of interest are those at 795 and 812.5 nm since imaging with these revealed that they originate from a circular area [indicated by arrows on Figs. 4(b) and 4(c)] centered on the mesa apex. Imaging with the mesa peaks at 740, 768, 785, and 806 nm revealed that they originate from sidewalls other than $\{110\}$ and present no further interest to the objective of this letter. Line scans at 795 and 812.5 nm obtained along a line passing through the mesa apex and parallel to a $[11\bar{2}]$ direction place the intensity maximum at the mesa apex [Fig. 4(d)]. TEM of all mesas studied revealed the four quantum wells to lie directly below the apex. The 795- and 812.5-nm emissions therefore originate from the mesa top wells. Although both these are "blue-shifted" compared to the bulk GaAs free-

exciton emission value of 820 nm, it is not evidence of 3D confinement. Unlike the claims of Ref. 3, a true quantum confinement arising from lateral size reduction requires a blue shift with respect to the emission from a well of equal thickness and laterally unconfined, as discussed next.

For the usual 1D confined GaAs (111)B quantum wells sandwiched between $\text{Al}_{0.2}\text{Ga}_{0.8}\text{As}$ barriers, an emission at 795 nm is calculated to originate from a 24 ML QW. The TEM observations on $0.6 \mu\text{m}$ mesas show the thicknesses of the four quantum wells to vary between 24 and 26 ML. Calculation of the energy states of the mesa top buffer SL layer with the peculiar well thickness variation was done using the measured layer thicknesses from TEM images of $0.6 \mu\text{m}$ mesas. The lowest transition ($e1-hh1$) is calculated to be at 814.3 nm. This agrees well with the observed peak at 812.5 nm. The observed red shift of the emission (795 nm) from the four mesa top quantum wells compared to the corresponding unpatterned peak (789 nm) indicates a net migration into the mesa top giving truncated pyramidal volumes of height higher than the 20 ML deposited (and found in the unpatterned region). Thus, both optical and structural (i.e., TEM) observations confirm migration to the mesa top. Although the TEM results clearly indicate the presence of four three-dimensionally confined volumes with the smallest volume corresponding to a pyramid with base 324 \AA and height of 65 \AA , the CL emission shows only one peak at 795 nm. This is a consequence of the tunneling time out of the smallest volume at the mesa top being very short compared to the radiative recombination time, the particle-hole pair generation probability being very small in the small volume, and the adjacent volumes offering lower energy states to thermalize into. The lateral dimensions of these three volumes being $\geq 1000 \text{ \AA}$, little lateral quantum size effects is expected. Clear emission from a *quantum* box of the size achieved here would be more readily observed if the lower AlGaAs barrier layer were made much thicker and preferably only a single quantum well grown. Efforts in this direction are underway.

This work was supported by the ARO, ONR, and AFOSR.

¹ *Nanostructure Physics & Fabrication*, edited by W. P. Kirk and M. A. Reed (Academic, New York, 1990).

² C. M. Sotomayor Torres, W. E. Leitch, D. Lootens, P. D. Wang, G. M. Williams, S. Thoms, H. Wallace, P. Van Daele, A. G. Cullis, C. R. Stanley, P. Deemester, and S. P. Beaumont in *Nanostructure and Mesoscopic Systems*, edited by W. Kirk and M. A. Reed (Academic, New York, 1992), p. 455.

³ T. Fukui and S. Ando, *Superlattices and Microstructures* **12**, 141 (1992).

⁴ A. Madhukar, K. C. Rajkumar, and P. Chen, *Appl. Phys. Lett.* **62**, 1547 (1993).

⁵ K. C. Rajkumar, K. Kaviani, J. Chen, P. Chen, A. Madhukar, and D. H. Rich, *Mater. Res. Soc. Proc.* **263**, 163 (1992).

⁶ S. Guha, A. Madhukar, L. Chen, K. C. Rajkumar, and R. M. Kapre, *SPIE Proc.* **1285**, 160 (1990).

⁷ P. Chen, K. C. Rajkumar, and A. Madhukar, *J. Vac. Sci. Technol. B* **9**, 2312 (1991).

⁸ K. C. Rajkumar, A. Madhukar, and P. Chen (unpublished).

⁹ W. T. Tsang and A. Y. Cho, *Appl. Phys. Lett.* **30**, 293 (1977).